NASA Technical Memorandum 102107

Unified Micromechanics of Damping for Unidirectional Fiber Reinforced Composites

D.A. Saravanos and C.C. Chamis
Lewis Research Center
Cleveland, Ohio

August 1989

NASA

UNIFIED MICROMECHANICS OF DAMPING FOR UNIDIRECTIONAL AND OFF-AXIS FIBER COMPOSITES

D. A. Saravanos, and C. C. Chamis*
National Aeronautics and Space Administration
Lewis Research Center
Cleveland, OH 44135

ABSTRACT

An integrated micromechanics methodology for the prediction of damping capacity in fiber-reinforced polymer matrix unidirectional composites has been developed. Explicit micromechanics equations based on hysteretic damping are presented relating the on-axis damping capacities to the fiber and matrix properties and volume fraction. The damping capacities of unidirectional composites subjected to off-axis loading are synthesized from on-axis damping values. Predicted values correlate satisfactorily with experimental measurements. The hygro-thermal effect on the damping performance of unidirectional composites due to temperature and moisture variations is also modeled. The damping contributions from interfacial friction between broken fibers and matrix are incorporated. Finally, the temperature rise in continuously vibrating composite plies is estimated. Application examples illustrate the significance of various parameters on the damping performance of unidirectional and off-axis fiber reinforced composites.

* *National Research Council - NASA Research Associate*

1. INTRODUCTION

The significance of material damping to the dynamic performance of structures is broadly recognized. Passive damping has been proved to be a significant design parameter for vibration control, fatigue endurance, and impact resistance. It is well known that fiber/polymer-matrix composites may provide one or two orders of magnitude higher material damping than common metals, in addition to other superior elastic properties, such as high specific moduli and specific strength. An additional appealing design factor is the possibility to tailor the composite damping, together with other mechanical properties, by controlling the anisotropy of the composite material. This combination of high damping and advanced mechanical characteristics makes fiber/polymer matrix composites materials ideal to a range of high-performance light-weight structures where passive vibration control is critical, such as space and aerospace structures, engine blades, high-speed mechanisms, etc.

In order to realize significant design benefits from the inherent damping capacity of composite materials, suitable mechanics theories should be formulated which will analytically correlate the damping of the composite structure to the properties of the basic constituents, ply stacking sequence, hygro-thermal conditions, existing damage, and structural configuration. Research at Lewis Center has led to the development of an integrated micromechanics theory for composite materials including the hygro-thermal (moisture, temperature) environmental effects [1]. The research has been being currently extended to incorporate prediction of damping. The current paper presents an integrated micromechanics theory for the on-axis and off-axis damping capacity of unidirectional composites.

Much but limited in scope research has been reported on the micromechanics of composite damping. Hashin [2] has provided analytical expressions for the on-axis ply damping, and Shultz and Tsai [3,4] have conducted experimental studies on the damping capacity of composite plies. Adams and co-workers [5-8], Bert and co-workers [9-10], and Gibson and co-workers [11-13] have performed analytical and experimental investigations on the micromechanics of composite damping. However, many reported theories on the microme-

chanics of composite damping have been mainly restricted to ply damping associated with the longitudinal normal stress σ_{l11} and/or the in-plane shear stress σ_{l12}. The current work presents a complete micromechanics theory for all 6 damping coefficients of a composite ply associated with the following local stresses: (1) longitudinal, (2) transverse, (3) through the thickness normal stress, (4) in-plane shear, (5) through the thickness (1-3) shear, and (6) through the thickness (2-3) shear. In contrast to many previous works which include only the hysteretic contribution of matrix, these six composite damping capacities are synthesized from the hysteretic damping of matrix and fibers, and interface friction. Isotropic dissipative properties are assumed for the matrix and anisotropic (but transversely isotropic) properties for the fibers. Temperature and moisture variations are known to have a significant impact on the properties of polymer matrix composites, hence, the influence of these two important factors on composite damping is modeled. In addition to hysteretic damping, the present method includes the contribution of interfacial friction damping due to broken fibers to the overall composite ply damping.

Off-axis specific damping capacities (SDC's), ie. the SDC's of a ply loaded at an off-axis angle, are also synthesized from the on-axis SDC's. The transformation for this purpose has been developed. Further, as a result of strain energy dissipation, temperature rise has been observed within vibrating plies [14]. Temperature variations affect the performance of composite materials, therefore, knowledge of the developed temperature profiles in vibrating composite plies is desirable. For this reason, the temperature rise in composite plies subjected to cyclic vibration is also predicted.

In the rest of the paper, the micromechanics for ply damping properties is described, application studies are presented, and most important conclusions are summarized.

NOMENCLATURE

A_d :	Area of debonded fiber.
d_f :	Fiber diameter.
E :	Normal modulus.
$[E_c]$:	Off-axis ply stiffness matrix.

$[E_l]$: On-axis ply stiffness matrix.

G : Shear modulus.

k : Volume ratio.

K : Thermal conductivity.

M : Moisture.

$\dot{q}$: Generated heat rate.

N_{fb} : Number of broken fibers through the ply thickness.

$[R_\sigma]$: Stress transformation matrix.

T : Temperature.

T_c : Temperature of composite at the center.

T_{cs} : Temperature of composite at the surface.

t : Ply thickness.

U : Stored strain energy per cycle.

u : Stored specific strain energy per cycle.

V : Volume.

δ_l : Effective fiber length.

δU : Dissipated strain energy per cycle.

δu : Dissipated specific strain energy per cycle.

ϵ : Engineering strain.

μ : Friction coefficient between fiber and matrix.

ν : Poisson's ratio.

σ : Stress.

ψ : Specific damping capacity.

ω : Forcing angular velocity.

Subscripts

c : Ply (off-axis).

D : Damping.

f : Fiber.

fr :	Fiber/matrix friction.
gd :	Glass transition, dry.
gw :	Glass transition, wet.
l :	Ply (on-axis).
m :	Matrix.
M :	Mechanical.
o :	Reference.
rad :	Radial.

Direction

11 :	Normal longitudinal.
22 :	Normal in-plane transverse.
33 :	Normal out-of-plane.
12 :	Shear in-plane.
23 :	Shear out-of-plane.
13 :	Shear out-of-plane.
xx :	In-plane normal, off-axis, x-direction.
yy :	In-plane normal, off-axis, y-direction.
ss :	In-plane shear, off-axis.
zz :	Normal, out-of-plane, z-direction.
n :	Normal.
s :	Shear.

2. COMPOSITE DAMPING

This section presents the damping micromechanics theory for continuous fiber composite material systems. In particular, the theory is focused on the damping of unidirectional composites subjected to : (1) on-axis cyclic loading, and (2) off-axis cyclic loading (ie. loading at an angle with respect to the fibers). The theory also addresses the impact of hygro-thermal effects and damage on the damping of composites.

The specific damping capacity (SDC) of a material is defined as the ratio of dissipated strain energy over the stored strain energy during one cycle of vibration.

$$\psi = \frac{\delta U}{U}$$

In the remaining section, the specific damping capacity (SDC) is consistently used, and all references to damping will imply SDC unless otherwise noted.

2.1. On-Axis Ply Damping

Fiber composites are nonhomogeneous materials, therefore, candidate sources of composite damping would be: (1) hysteretic damping in the polymer matrix, (2) hysteretic damping in the fibers, and (3) friction damping at the fiber-matrix interface as a result of bonding imperfections, broken fibers, or debonding. Most available theories on the micromechanics of composite damping have mainly provided closed-form solutions for the ply damping associated with the longitudinal normal stress σ_{l11} and the in-plane shear stress σ_{l12}. The current work presents simple explicit expressions of ply SDC's associated with all 6 engineering stresses illustrated in Figure 1a, namely, the normal longitudinal stress σ_{l11}, normal transverse stress σ_{l22}, normal through- the-thickness stress σ_{l33}, in-plane shear stress σ_{l12}, and out-of-plane shear stresses σ_{l23} and σ_{l13}.

For fiber/polymer matrix composites, the damping capacity of the matrix is usually significantly higher than the damping capacity of the fibers, for this reason, many micromechanics theories [2,5-7] have neglected the contribution of fiber damping. This assumption, may be satisfactory for the transverse normal or shear specific damping capacities, but is certainly less accurate for the longitudinal normal damping. Moreover, aramid fibers typically exhibit longitudinal SDC about 1.8%, which is not negligible compared to reported SDC values for epoxies. In order to remedy this discrepancy, the presented micromechanics theory includes the contribution of the fibers into the damping of the composite.

Another drawback of most micromechanics theories is their restriction to fibers and matrix with isotropic elastic and dissipative properties. In general, this hypothesis is incorrect, especially for carbon/graphite fibers. The present theory remedies also this

restriction by assuming linear anisotropic viscoelastic properties for the fibers and linear isotropic viscoelastic properties for the polymer matrix. Experimental work on glass and carbon composites [6] has shown low dependence of composite damping to the strain values, indicating that the latter assumption would be a reasonable approximation for most engineering applications. The present micromechanics theory assumes square packing arrays of fibers as this type of packing represents the average value of randomly distributed fibers. Nevertheless, if necessary, similar micromechanics theories can be developed for other packing patterns.

Longitudinal Normal Damping. The square array of a ply consists of one fiber and the surrounding matrix, as shown in Figure 1a. Assuming that a uniform cyclic longitudinal normal stress of amplitude σ_{l11} is applied to the ply, then the dissipated strain energy within the representative fiber/matrix segment would be:

$$\delta U_{l11} = \frac{1}{2}\int_{V_f} \psi_{f11}\sigma_{f11}\epsilon_{f11}dV_f + \frac{1}{2}\int_{V_m} \psi_{mn}\sigma_{mn}\epsilon_{mn}dV_m \tag{1}$$

Because damping is assumed to be independent of stress and strain,

$$\delta U_{l11} = \frac{1}{2}\psi_{f11}\int_{V_f} \sigma_{f11}\epsilon_{f11}dV_f + \frac{1}{2}\psi_{mn}\int_{V_m} \sigma_{mn}\epsilon_{mn}dV_m \tag{2}$$

The longitudinal SDC ψ_{l11} is defined as:

$$\delta U_{l11} = \psi_{l11}U_{l11} \tag{3}$$

Further, the stored strain energy during one vibration cycle will be

$$U_{l11} = \frac{1}{2}\int_{V_f} \sigma_{f11}\epsilon_{f11}dV_f + \frac{1}{2}\int_{V_m} \sigma_{mn}\epsilon_{mn}dV_m = \frac{1}{2}\int_{V_l} \sigma_{l11}\epsilon_{l11}dV_l \tag{4}$$

The last equation represents the rule of mixtures in strain energy form. It should be recognized that based on the assumed stress/strain uniformity, equation (4) leads to the broadly accepted rule of mixtures for the longitudinal modulus:

$$E_{l11} = k_f E_{f11} + k_m E_m \tag{5}$$

Combination of equations (2), (3), and (4) will provide the following expression for longitudinal SDC,

$$\psi_{l11} = \psi_{f11} k_f \frac{E_{f11}}{E_{l11}} + \psi_{mn} k_f \frac{E_m}{E_{l11}} \tag{6}$$

Transverse Normal Damping. If a cyclic transverse normal stress of amplitude σ_{l22} is applied to the constitutive fiber/matrix section of Figure 1a, then the dissipated and stored strain energy during a vibration cycle may be similarly described by:

$$\delta U_{l22} = \frac{1}{2} \int_{V_f} \psi_{f22} \sigma_{f22} \epsilon_{f22} dV_f + \frac{1}{2} \int_{V_m} \psi_{mn} \sigma_{mn} \epsilon_{mn} dV_m \tag{7}$$

and

$$U_{l22} = \frac{1}{2} \int_{V_f} \sigma_{f22} \epsilon_{f22} dV_f + \frac{1}{2} \int_{V_m} \sigma_{mn} \epsilon_{mn} dV_m \tag{8}$$

The stress distribution in the matrix and fiber is not uniform mainly due to the curvature of the fiber, however, uniform stress distributions may be assumed within the fiber and matrix provided that the shape and the volume of the fiber are properly corrected. This approach has been successfully utilized by Chamis [15] in the development of micromechanics equations for the transverse and shear elastic moduli E_{l11}, E_{l22}, E_{l33}, G_{l12}, G_{l13}, and G_{l23} which are also used herein. The validity of the assumption has been verified by three-dimensional finite element analysis [16]. Combination of equations (7) and (8) results in the following equation for the transverse normal SDC of the composite:

$$\psi_{l22} = \psi_{f22} \sqrt{k_f} \frac{E_{22}}{E_{f22}} + \psi_{mn} (1 - \sqrt{k_f}) \frac{E_{22}}{E_m} \tag{9}$$

where,

$$E_{22} = (1 - \sqrt{k_f}) E_m + \frac{\sqrt{k_f} E_m}{1 - \sqrt{k_f} (1 - \frac{E_m}{E_{f22}})} \tag{10}$$

Because of the transverse isotropy of the fibers, and consequently of the composite material, the transverse damping capacity of the ply along the material 3-axis would be,

$$\psi_{l33} = \psi_{l22} \tag{11}$$

In-Plane Shear Damping. Based on the same assumptions and following a similar procedure as in case of transverse damping, the in-plane shear damping capacity is given by:

$$\psi_{l12} = \psi_{f12}\sqrt{k_f}\frac{G_{12}}{G_{f12}} + \psi_{ms}(1-\sqrt{k_f})\frac{G_{12}}{G_m} \tag{12}$$

where,

$$G_{12} = (1-\sqrt{k_f})G_m + \frac{\sqrt{k_f}G_m}{1-\sqrt{k_f}(1-\frac{G_m}{G_{f12}})} \tag{13}$$

Through-the-Thickness Shear Damping. Due to the transverse isotropy of the composite ply, the interlaminar SDC ψ_{l13} is equal to the in-plane SDC of the ply,

$$\psi_{l13} = \psi_{l12} \tag{14}$$

An analogous approach also provides the out-of-plane shear SDC ψ_{l23},

$$\psi_{l23} = \psi_{f23}\sqrt{k_f}\frac{G_{l23}}{G_{f23}} + \psi_{ms}(1-\sqrt{k_f})\frac{G_{l23}}{G_m} \tag{15}$$

where,

$$G_{l23} = \frac{E_{l22}}{2(1+\nu_{l23})} \tag{16}$$

$$\nu_{l23} = \frac{\nu_m}{1-k_f\nu_m} + k_f(\nu_{f23} - \frac{(1-k_f)\nu_m}{1-k_f\nu_m}) \tag{17}$$

2.2. Hygro-Thermal Effect

Variations in the temperature and moisture content of a polymer matrix composite will primarily affect the properties of the plastic matrix. Previous studies [17] have shown that the hygro-thermal impact on most mechanical properties of the matrix can be expressed as,

$$\frac{P_M}{P_o} = [\frac{T_{gw}-T}{T_{gd}-T_o}]^{0.5} \tag{18}$$

Based on the fact that for temperature ranges below the glass transition the matrix damping is increasing with temperature, an inversed form of equation (18) is proposed for the hygro-thermal effect on the matrix damping:

$$\frac{P_D}{P_o} = [\frac{T_{gd}-T_o}{T_{gw}-T}]^q \tag{19}$$

The wet glass transition temperature is,

$$T_{gw} = T_{gd}(0.005M_l^2 - 0.1M_l + 1) \tag{20}$$

The exponent q can be easily correlated to experimental data of each individual polymer matrix. In this study, the value q=0.5 is assumed. The hygro-thermal effect on the ply properties is related to the effect on the matrix via the micromechanics equations of Section 2.1. The hygro-thermal effects are expected to dominate the transverse and shear damping properties of a ply, as they are predominantly controlled by the matrix. The results presented in Section 3 illustrate this trend.

2.3. Off-Axis Ply Damping

During off-axis cyclic loading (Figure 1b), more than one of the on-axis SDC's will contribute to the overall ply damping. Based on this observation, one may anticipate that the off-axis ply damping will be related to both on-axis damping properties and the orientation of the fibers. A transformation law has been derived to describe this relationship based on the fact that strain energy loss is invariant to stress/strain transformations.

By definition, the hysteretic strain energy loss per unit volume in the structural (off-axis) coordinate system is,

$$\delta u = \frac{1}{2}\{\sigma_c\}^T[\psi_c]\{\epsilon_c\} \tag{21}$$

while in the material (on-axis) coordinate system it will be:

$$\delta u = \frac{1}{2}\{\sigma_l\}^T[\psi_l]\{\epsilon_l\} \tag{22}$$

Transforming the stress and strain from the material coordinate system to the structural coordinate system, the specific strain energy loss becomes,

$$\delta u = \frac{1}{2}\{\sigma_c\}^T[R_\sigma]^T[\psi_l][R_\sigma^{-1}]^T\{\epsilon_c\} \tag{23}$$

The stress transformation matrix $[R_\sigma]$ is given in Appendix. Equating the right hand sides of equations (21) and (23) the following ply damping transformation law results,

$$[\psi_c] = [R_\sigma]^T[\psi_l][R_\sigma^{-1}]^T \tag{24}$$

In the previous expression the on-axis damping matrix is diagonal:

$$[\psi_l] = \begin{bmatrix} \psi_{l11} & 0 & 0 \\ 0 & \psi_{l22} & 0 \\ 0 & 0 & \psi_{l12} \end{bmatrix} \tag{25}$$

while the off-axis ply damping is fully populated.

$$[\psi_c] = \begin{bmatrix} \psi_{cxx} & \psi_{cxy} & \psi_{cxs} \\ \psi_{cyx} & \psi_{cyy} & \psi_{cys} \\ \psi_{csx} & \psi_{csy} & \psi_{css} \end{bmatrix} \tag{26}$$

The non-diagonal terms indicate coupling between the axial and shear stresses. Apparently, off-axis loading will affect the overall damping capacity of a ply in two distinct ways: (1) by altering the values of the diagonal terms, which is equivalent to altering the dissipative capability of the ply directly associated to normal and shear strain, and (2) by inducing and altering non-diagonal terms, which control the amount of strain energy dissipated by coupled deformation modes.

2.4. Interfacial Friction Damping

Relative motion between broken debonded fibers and the surrounding matrix is the source for additional frictional damping in a composite. During one vibration cycle, friction will be developed between the debonded fiber and matrix when the radial stress σ_{rad} is compressive. The dissipated energy per cycle from a debonded fiber will be:

$$\delta U_{fr} = \oint (\int_{A_d} |\mu \sigma_{rad} d\epsilon_{l11} r| dA_d) \tag{27}$$

where, μ is the friction coefficient between fiber and matrix, σ_{rad} the average radial stress around the fiber, and r the distance from the point where debonding starts. The area of debonded fiber A_d is

$$A_d = \pi d_f \delta_l \tag{28}$$

where δ_l is the effective fiber length [18],

$$\delta_l = 1.15 d_f [\frac{1 - \sqrt{k_f}}{\sqrt{k_f}} (\frac{E_{f11}}{G_m})]^{0.5} \tag{29}$$

For N_{fb} broken fibers through the thickness, the specific energy loss per cycle will be:

$$\delta u_{fr} = \frac{N_{fb}\delta U_{fr}}{t_l \delta_l d_f \sqrt{\frac{\pi}{4k_f}}} \tag{30}$$

Integration of equation (27) over the surface of the debonded fiber, and combination of equations (27-30) will lead to the following equation for the specific strain energy loss per cycle due to friction:

$$\delta u_{fr} = \sqrt{\pi k_f}\mu N_{fb}\frac{\delta_l}{t_l}\oint |\sigma_{rad} d\epsilon_{l11}| \tag{31}$$

For sinusoidal stressing equation (31) becomes,

$$\delta u_{fr} = \sqrt{\pi k_f}\mu N_{fb}\frac{\delta_l}{t_l}\oint \sigma_{rad}\epsilon_{l11}|sin(\omega t)d(sin(\omega t))| \tag{32}$$

Taking into consideration that friction exists only when $\sigma_{rad} < 0$, equation (32) reduces to:

$$\delta u_{fr} = \sqrt{\pi k_f}\mu N_{fb}\frac{\delta_l}{t_l}\sigma_{rad}\epsilon_{l11} \tag{33}$$

The total SDC of a ply may be ensembled from the frictional loss and the hysteretic loss described in equations (21-22). When only longitudinal stress is applied on the ply, the equivalent longitudinal friction damping will be,

$$\psi_{l11,fr} = 2\sqrt{\pi k_f}\mu N_{fb}\frac{\delta_l}{t_l}\frac{\sigma_{rad}}{\sigma_{l11}} \tag{34}$$

Based on a previous micromechanics analysis reported by Chamis [19], the radial stress is related to the ply microstresses. As shown in ref. [19], ply microstresses are directly related to mechanical ply stresses, temperature variations, and moisture variations, therefore, the current analysis for composite friction damping readily incorporates the effect of mechanical loads, residual thermal microstresses, and hygral microstresses.

2.5. Temperature Rise

As a result of damping, a portion of stored strain energy is lost and is converted to heat during the vibration of the composite. The generated heat is transferred to the surrounding environment and temperature gradients are developed in the material. During continuous dynamic excitation, significant temperature rise may occur within the composite. As stated in the previous section, the mechanical and thermal properties of polymer matrix composites are temperature dependent, hence, as the temperature increases, the mechanical and thermal properties of the composite, as well as, the generated heat continuously change. In case of a steady-state excitation, the composite will eventually reach thermal and vibrational stability. The actual temperature rise depends on the SDC of the composite material, the conductivities of the composite material and surrounding media, the laminate configuration, and the induced excitation power. Fourier's law may be utilized to estimate the steady-state temperature rise. For plies of infinite dimensions being subjected to steady-state excitation,

$$\frac{\partial}{\partial z}(K_{zz}(T)\frac{\partial T}{\partial z}) + \dot{q}(T) = 0 \tag{35}$$

For cyclic excitation, the heat generation rate is described by equation (22) for unidirectional composites or by equation (21) for off-axis composites. Solutions are provided for the mid-surface temperature T_c assuming equal temperatures T_{cs} at both surfaces of the composite.

On-axis loading:

$$\delta(T_c - T_{cs}) = \frac{\omega t_c^2}{16 K_{l33}} \{\sigma_l\}^T [\psi_l] [E_l]^{-1} \{\sigma_l\} \tag{36}$$

Off-axis loading:

$$\delta(T_c - T_{cs}) = \frac{\omega t_c^2}{16 K_{czz}} \{\sigma_c\}^T [\psi_c] [E_c]^{-1} \{\sigma_c\} \tag{37}$$

3. DISCUSSION OF RESULTS

Results are presented in this section for various composite systems. Whenever possible, the predicted values are compared to available experimental data. It is pointed out, however, that limited experimental data has been reported correlating constituent damping properties to ply damping (on-axis or off-axis). In the following applications experimental measurements performed by Adams and co-workers [5-8,20] are utilized.

3.1. On-Axis Ply Damping

Figures 2, 3, 4 and 5 demonstrate the variation of longitudinal SDC ψ_{l11}, in-plane shear SDC ψ_{l12}, transverse SDC ψ_{l22}, and out-of-plane SDC ψ_{l23} with respect to the fiber volume ratio. The different curves represent different fiber/matrix combinations. The ply SDC's have been normalized by the normal or shear SDC of the matrix. The SDC's for the intermediate modulus high strength (IMHS) matrix and intermediate modulus low strength (IMLS) matrix are shown in Table 1, and they represent values for DX210 epoxy and polyester respectively, provided in Refs. [5,8]. Non-reported fiber/matrix SDC's were backcalculated from on-axis composite damping data reported in reference [7].

As seen in Figure 2, the agreement between analytical predictions and experimental measurements for longitudinal SDC is good. For E-Glass/IMLS the agreement is excellent. The predicted values for the high modulus surface treated graphite/polyester (HMS/IMLS) underestimate the experimental ones, but an uncertainty exists about the actual values of the fiber properties. In Figure 3, the analytical predictions for shear in-plane SDC overpredict the measured values for the glass fiber, but they are in acceptable agreement for the graphite fiber. The same comments apply for the correlation of transverse SDC with experimental data in Figure 4. Overall, the present micromechanics theory has yielded acceptable damping predictions for fiber volume ratios within the range of interest to most engineering applications. The study has also revealed the need for systematic collection of experimental data regarding on-axis composite damping. Also, the present micromechanics is expected to yield better understanding regarding the design of suitable experiments for measuring composite damping.

The longitudinal damping is fiber controlled, while the transverse and shear damping

are matrix controlled. The fibers have also significant impact on the transverse and shear ply damping, as they control the amount of strain energy stored in the matrix. The fiber effect is clearly demonstrated in Figures 2,3,4 and 5. In general, fibers with high moduli will decrease the damping of the ply, as they will reduce the amount of strain energy stored in the matrix and hence the overall dissipated strain energy.

3.2. Hygro-Thermal Effect on Ply Damping

The hygro-thermal effect on the longitudinal, in-plane shear, and transverse SDC's is shown in Figures 6, 7, and 8 respectively for an HM-S/IMHS composite system. The various curves represent different temperature/moisture increments above the reference values. The matrix glass transition temperature is 420 degrees F, the reference temperature 70 degrees F, and the reference moisture content 0%. The longitudinal SDC has shown insensitivity to temperature and moisture variation, because it is mainly a fiber controlled property. However, the transverse and shear SDC's indicate dramatic dependence to temperature or moisture variations. The combined effect of temperature and moisture is also illustrated in the same Figures. The out-of-plane shear SDC ψ_{l23} has shown analogous hygro-thermal dependence.

3.3. Off-Axis Ply Damping

The predicted values for off-axis SDC's are shown in Figure 9 for a 50% fiber volume fraction HM-S/DX210 graphite/epoxy ply. For a coherent assessment on the accuracy of the transformation law, the on-axis SDC's were assumed equal to those measured by Ni and Adams [20]. These damping measurements were conducted on cantilever off-axis composite plate beams harmonically excited at their first bending vibration mode. Thus, the measured values represent the modal damping at individual vibration modes and include the effect of coupling terms. Therefore, it is appropriate to compare the measured values with the equivalent axial ply SDC $\psi_{x,axial}$ defined as the combined damping capacity of plies subjected to a single cyclic normal stress σ_{cxx}. The axial damping includes the coupling effect and its calculation is straight forward by utilizing equation (21) and Hook's law (equation (A3) in Appendix) for the ply. The resultant axial damping ($\psi_{x,axial}$) values

vs. the fiber angle θ are plotted in Figure 9 and are in excellent agreement with the experimental results. The remaining error has been attributed to the fact that global modal damping is compared to predicted local values. Overall, the agreement of the damping transformation is very good.

The diagonal SDC terms in Equation (26) ψ_{cxx}, ψ_{cyy}, and ψ_{css} are also plotted as functions of the fiber angle θ in Figure 9. The normal SDC is minimum at 0 degrees and maximum near 60 degrees, while the shear SDC is symmetric being maximum at 0 and 90 degrees and minimum at 45 degrees. Figure 9 also vividly demonstrates the effect of coupling damping terms on the axial damping capacity of an off-axis ply. Coupling damping terms are the predominant source of axial damping for ply angles between 5 and 30 degrees and their contribution progressively decreases for ply angles greater than 30 degrees.

3.4. Friction Effect on Ply Damping

The interfacial friction damping contribution due to broken fibers is shown in Figure 10. Figure 10 illustrates the increase in longitudinal SDC vs. the fiber volume fraction for various percentages of broken fibers of a 0.02in thick HM-S/IMHS unidirectional composite subject to unidirectional cyclic stress σ_{l11} of 20 ksi amplitude. The effect of any thermal curing residual microstresses was neglected, although this capability readily exists in the method, in order to assess the effect of pure mechanical loads on the friction damping. The coefficient of friction between fiber and matrix was assumed to be 0.30. Although the friction effect is comparable to the hysteretic damping values, the resultant friction damping is rather low due to the small radial stress involved in longitudinal loading.

In the case of off-axis loading, the friction damping will be higher because the transverse and shear stresses will increase the radial stress. The trend is illustrated in Figure 11 where the axial SDC's of two 50% HM-S/IMHS off- axis plies, the first without broken fibers and the second with 20% broken fibers, are plotted as functions of the ply angle. Both plies are excited by a cyclic axial stress σ_{cxx}. Interestingly, the friction damping is low at 0 degrees, then increases and peeks near 25 degrees, is reduced again to zero as the

longitudinal strain is reduced due to Poisson's effect, and then is increased again. At fiber angles near 90 degrees, the friction damping is mainly induced by the Poisson's effect.

3.5. Temperature Rise

The temperature rise at the outer surface and mid-plane of a 0.04in, 50% HT-S/IMHS unidirectional composite, excited by a sinusoidal uniaxial off-axis stress σ_{cxx}, with 10 ksi amplitude and 50 Hz frequency, is shown in Figure 12 for various off-axes angles. The surrounding media of the composite is assumed to be motionless air with convection rate 0.007 $BTU/(hr-in^2-^oF)$. The actual convection rate around a vibrating composite would be higher, hence, Figure 12 presents an upper bound for the temperature rise. Estimation of the actual heat convection rate is beyond the scope of the paper, but regardless of this issue, a significant temperature rise is predicted as the off-axis angle is increased. Consequently, variations in the elastic and damping characteristics of composite plies should be expected in off-axis cyclic loading. In view of the sensitivity of composite damping to temperature variations, differences in predicted and measured values for composite damping in off-axis cyclic loading may occur.

4. SUMMARY

A unified micromechanics theory for the damping capacity of composites has been presented. The theory includes simple approximate equations for synthesizing specific damping capacities based on: (1) elastic and dissipative constituent properties, (2) interface properties, (3) ply temperature and moisture, (4) off-axis loading, and (5) temperature rise due to continuous vibration. The micromechanics theory has been augmented into the ICAN computer code [1].

Predicted results compare well with available experimental measurements reported in open literature. The correlation has added confidence to the validity of the theory, but additional experimental work is needed in some areas. The results illustrate the following important trends regarding the specific damping capacity (SDC) of composite materials:

i. The longitudinal on-axis SDC is controlled by the fibers and is rather insensitive to fiber volume fractions of practical interest. All other SDC's are predominantly

controlled by matrix and are sensitive to fiber volume ratio. The fiber moduli also influence the SDC of the composite, in that, they control the distribution of strain energy into the matrix. In view of this wide sensitivity of composite damping to micromechanics parameters, the present theory is a valuable approach for selecting suitable fiber/matrix combinations and fiber volume ratios in order to satisfy particular damping requirements.

ii. Off-axis ply SDC's have demonstrated wide variation with respect to fiber angle, indicating that ply angles may be an effective design parameter for tailoring the damping capacity of composite plies.

iii. Temperature and moisture variations have shown significant influence on the damping capacity of composite plies.

vi. The temperature rise within continuously vibrating composite plies was found significant for off-axis loading and disproportional to the respective ply damping. The latter observation indicates that the issue of temperature rise requires special design consideration, since it significantly influences the damping capacity.

v. Interfacial friction damping contributes to the overall damping capacity of unidirectional composites and its contribution is more significant in case of off-axis loading.

REFERENCES

1. Murthy, P. L. N. and Chamis, C. C., "ICAN: Integrated Composites Analyzer," *AIAA Paper 84-0974,* May 1984.

2. Hashin, Z., "Complex Moduli of Viscoelastic Composites—II. Fiber Reinforced Composite Materials," *International Journal of Solids and Structures,* Vol. 6, No. 6, June 1970, pp. 797–807.

3. Schultz, A. B. and Tsai, S. W., "The Dynamic Moduli and Damping Ratios in Fibre Reinforced Composites," *Journal of Composite Materials,* Vol. 2, No. 3, July 1968, pp. 368–379.

4. Schultz, A. B. and Tsai, S. W., "Measurements of Complex Dynamic Moduli for Laminated Fibre-Reinforced Composites," *Journal of Composite Materials,* Vol. 3, 1969, pp. 434–443.

5. Adams, R. D., Fox, M. A. O., Flood, R. J. L., Friend, R. J., and Hewitt, R. L., "The Dynamic Properties of Unidirectional Carbon and Glass Fibre-Reinforced Plastics in Torsion and Flexure," *Journal of Composite Materials,* Vol. 3, 1969, pp. 594–603.

6. Adams, R. D. and Bacon, D. G. C., "Measurement of the Flexural Damping Capacity and Dynamic Young's Modulus of Metals and Reinforced Plastics," *Journal of Physics, D: Applied Physics,* Vol. 6, No. 1, Jan. 1973, pp. 27–41.

7. Adams, R. D. and Bacon, D. G. C., "Effect of Fibre Orientation and Laminate Geometry on the Dynamic Properties of CFRP," *Journal of Composite Materials,* Vol. 7, Oct. 1973, pp. 402–428.

8. Ni, R. G. and Adams, R. D., "A Rational Method for Obtaining the Dynamic Mechanical Properties of Laminae for Predicting the Stiffness and Damping of Laminated Plates and Beams," *Composites,* Vol. 15, No. 3, July 1984, pp. 193–199.

9. Chang, S. W. and Bert, C. W., "Analysis of Damping for Filamentary Composite Materials, *Composite Materials in Engineering Design, B. R. Noton, ed., American Society for Metals,* Metals Park, 1973, pp. 51–62.

10. Siu, C. C. and Bert, C. W., "Sinusoidal Response of Composite-Material Plates with Material Damping," *Journal of Engineering for Industry,* Vol. 96, no. 2, May 1974, pp. 603–610.

11. Gibson, R. F. and Plunkett, R., "Dynamic Mechanical Behavior of Fibre-Reinforced Composites: Measurement and Analysis," *Journal of Composite Materials,* Vol. 10, No. 4, Oct. 1976, pp. 325–341.

12. Sun, C. T., Chaturvedi, S. K., and Gibson, R. F., "Internal Damping of Short-Fiber Reinforced Polymer Matrix Composites," *Computers and Structures,* Vol. 20, No. 1–3, 1985, pp. 391–400.

13. Suarez, S.A., Gibson, R. F., Sun, C. T., and Chaturvedi, S. K., "The Influence of Fiber Length and Fiber Orientation on Damping and Stiffness of Polymer Composite Materials," *Experimental Mechanics,* Vol. 26, No. 2, June 1986, pp. 175–184.

14. Daniel, I. M. and Liber, T., "Lamination Residual Stresses in Fiber Composites," *NASA CR-134826,* 1975.

15. Chamis, C. C., "Simplified Composite Micromechanics Equations for Hygral, Thermal, and Mechanical Properties," *SAMPE Quarterly,* Vol. 15, No. 3, April 1984, pp. 14-23.

16. Caruso, J. J. and Chamis, C. C., "Assessment of Simplified Composite Micromechanics Using Three-Dimensional Finite-Element Analysis," *Journal of Composites Technology and Research,* Vol. 8, No. 3, Fall 1986, pp. 77-83.

17. Chamis, C. C., Lark, R. F., and Sinclair, J. H., "Integrated Theory for Predicting the Hydrothermomechanical Response of Advanced Composite Structural Components," *Advanced Composite Materials—Environmental Effects,* J. R. Vinson, ed., ASTM STP-658, American Society for Testing and Materials, Philadelphia, PA, 1978, pp. 160-192.

18. Chamis, C. C., "Micromechanics Strength Theories, *Fatigue and Fracture,* Vol. 5, L. J. Broutman, ed., Academic Press, 1974, pp. 93-151.

19. Chamis, C. C., "Simplified Composite Micromechanics for Predicting Microstresses," *Journal of Reinforced Plastics and Composites,* Vol. 6, No. 3, July 1987, pp. 268-289.

20. Ni, R. G. and Adams, R. D., "The Damping and Dynamic Moduli of Symmetric Laminated Composite Beams—Theoretical and Experimental Results," *Journal of Composite Materials,* Vol. 18, No. 2, Mar. 1984, pp. 104-121.

APPENDIX

On-axis ply stiffness:

$$\{\sigma_l\} = [E_l]\{e_l\} \tag{A1}$$

$$[E_l]^{-1} = \begin{bmatrix} \frac{1}{E_{l11}} & -\frac{\nu_{l21}}{E_{l22}} & 0 \\ -\frac{\nu_{l21}}{E_{l11}} & \frac{1}{E_{l22}} & 0 \\ 0 & 0 & \frac{1}{G_{l12}} \end{bmatrix} \tag{A2}$$

Off-axis ply stiffness:

$$\{\sigma_c\} = [E_c]\{e_c\} \tag{A3}$$

$$[E_c]^{-1} = [R_\sigma]^T [E_l]^{-1} [R_\sigma] \tag{A4}$$

$$[R_\sigma] = \begin{bmatrix} cos^2\theta & sin^2\theta & sin2\theta \\ sin^2\theta & cos^2\theta & -sin2\theta \\ -0.5sin2\theta & 0.5sin2\theta & cos2\theta \end{bmatrix} \tag{A5}$$

$$[E_c]^{-1} = \begin{bmatrix} \frac{1}{E_{cxx}} & -\frac{\nu_{cyx}}{E_{cyy}} & \frac{\nu_{csx}}{G_{cxy}} \\ -\frac{\nu_{cxy}}{E_{cxx}} & \frac{1}{E_{cyy}} & \frac{\nu_{csy}}{G_{cxy}} \\ \frac{\nu_{cxs}}{E_{cxx}} & \frac{\nu_{cys}}{E_{cyy}} & \frac{1}{G_{cxy}} \end{bmatrix} \tag{A6}$$

Table 1 Specific damping capacities for matrix and fibers.

Matrix	ψ_{mn} (%)	ψ_{ms} (%)
IMLS (Polyester)	8.5	13.8
IMHS (Epoxy)	6.6	6.9

Fiber	ψ_{f11} (%)	ψ_{f22} (%)	ψ_{f12} (%)	ψ_{f23} (%)
E-Glass	1.1	1.1	0.6	0.6
HT-S	0.7	0.7	0.6	0.6
HM-S	1.0	1.0	1.0	1.0

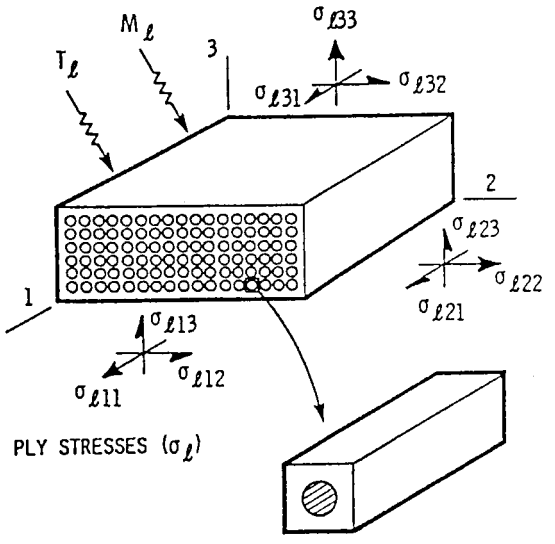

(a) ON-AXIS.

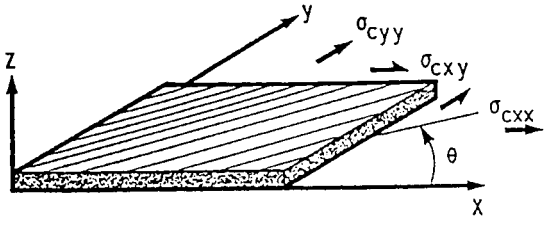

(b) OFF-AXIS.

FIGURE 1. - TYPICAL CONTINUOUS FIBER COMPOSITE PLIES.

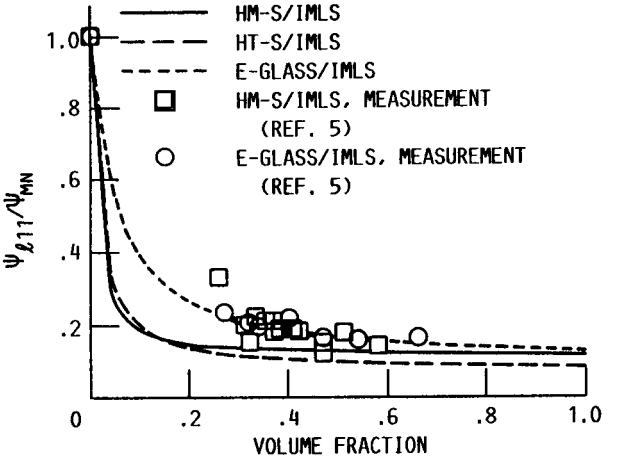

FIGURE 2. - LONGITUDINAL NORMAL SPECIFIC DAMPING CAPACITY.

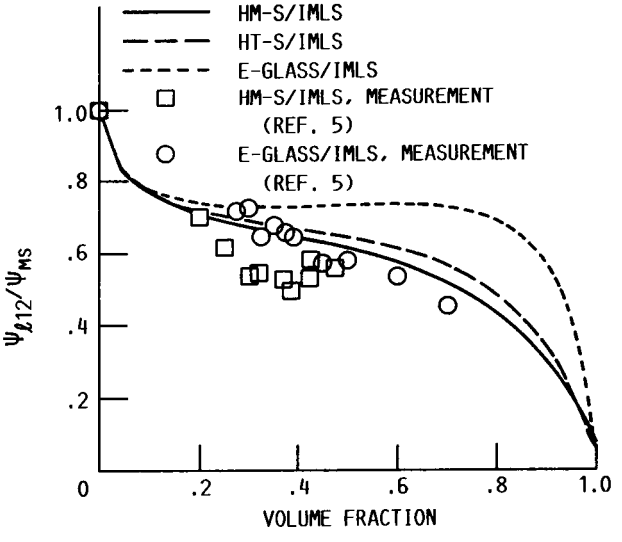

FIGURE 3. - IN-PLANE SHEAR SPECIFIC DAMPING CAPACITY.

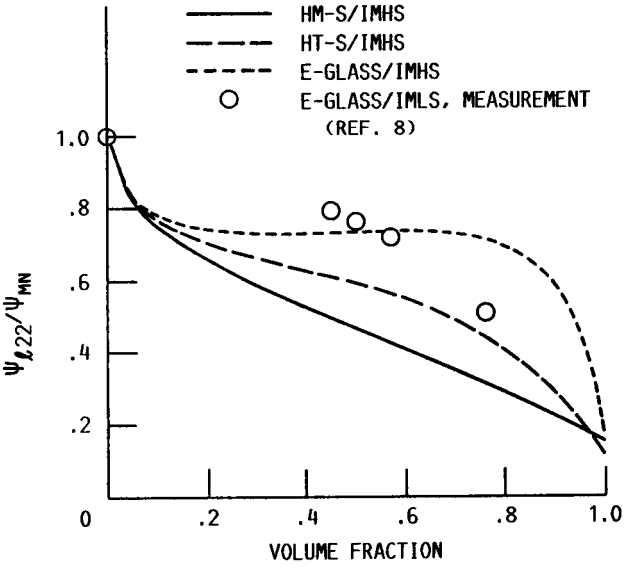

FIGURE 4. - TRANSVERSE NORMAL SPECIFIC DAMPING CAPACITY.

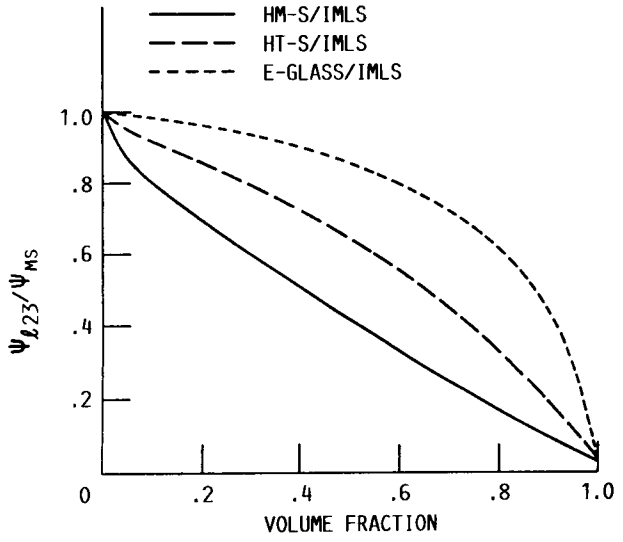

FIGURE 5. - THROUGH-THE-THICKNESS SHEAR SPECIFIC DAMPING CAPACITY.

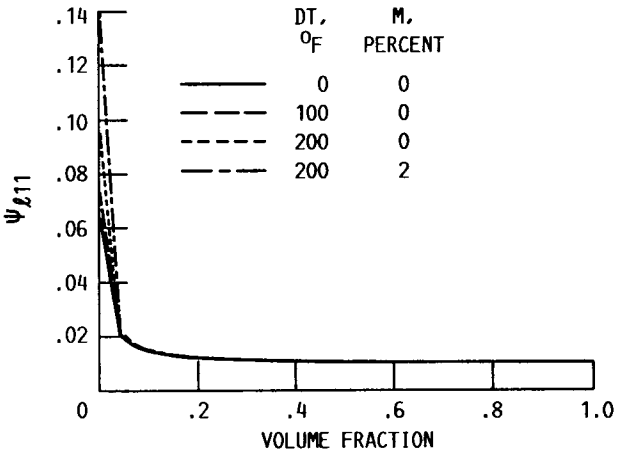

FIGURE 6. - HYGROTHERMAL EFFECT ON LONGITUDINAL NORMAL DAMPING. HM-S/IMHS GRAPHITE-EPOXY.

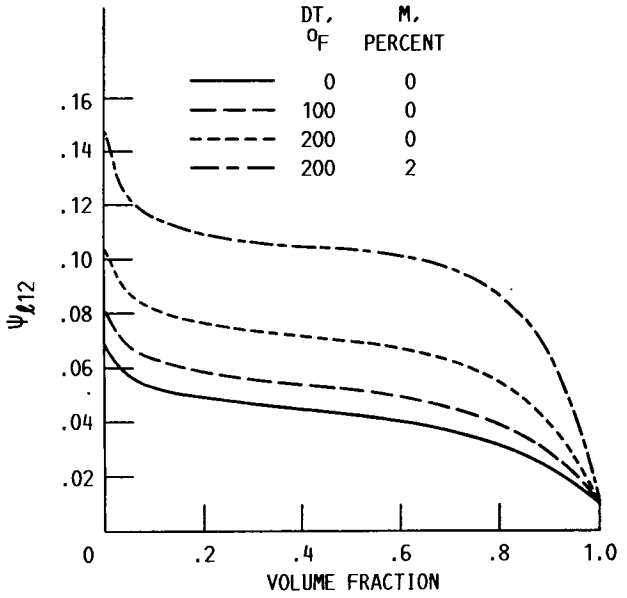

FIGURE 7. - HYGROTHERMAL EFFECT ON IN-PLANE SHEAR DAMPING. HM-S/IMHS GRAPHITE-EPOXY.

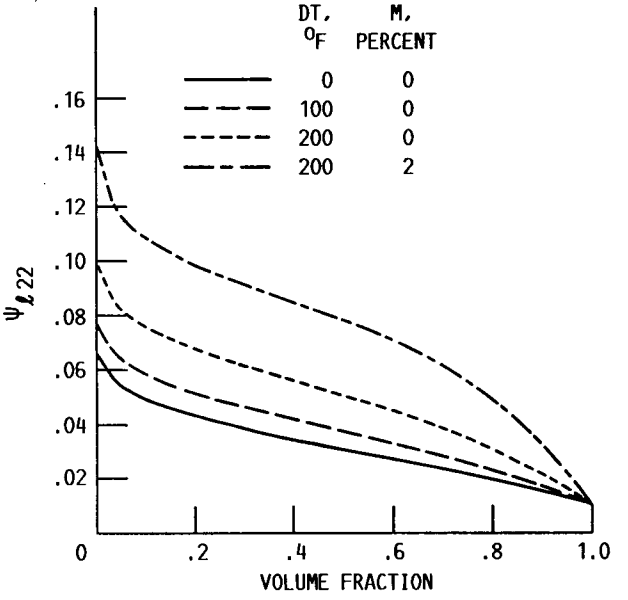

FIGURE 8. - HYGROTHERMAL EFFECT ON TRANSVERSE NORMAL DAMPING. HM-S/IMHS GRAPHITE-EPOXY.

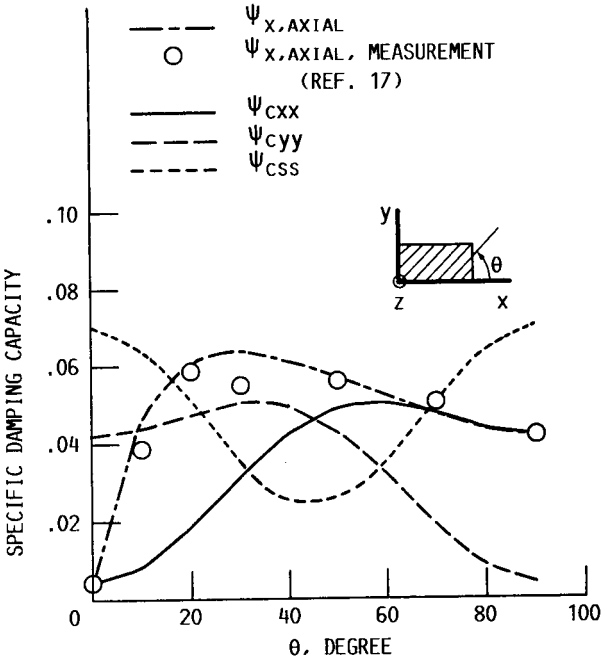

FIGURE 9. - SPECIFIC DAMPING CAPACITIES OF A 50 PERCENT HM-S/DX210 OFF-AXIS COMPOSITE.

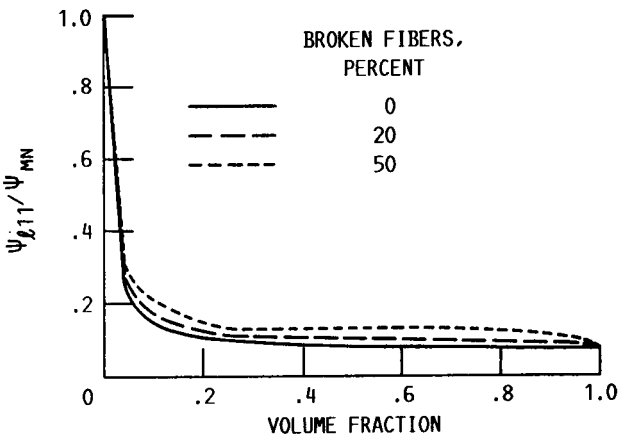

FIGURE 10. - EFFECT OF FRICTION DAMPING ON THE ON-AXIS LONGITUDINAL SDC OF A HM-S/IMHS COMPOSITE.

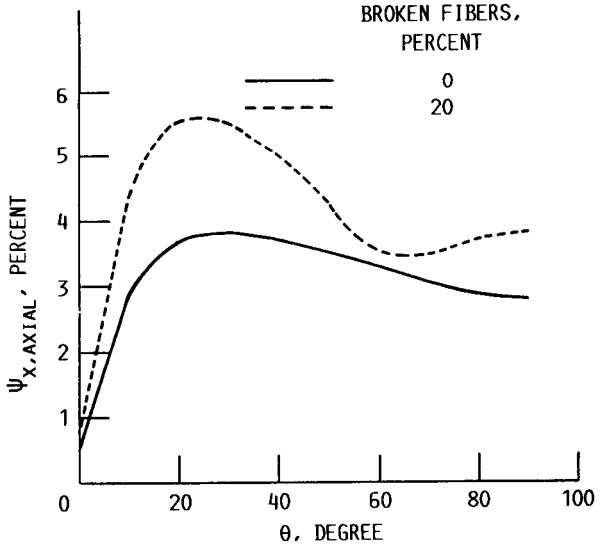

FIGURE 11. - EFFECT OF FRICTION DAMPING ON THE AXIAL SDC OF A 50 PERCENT HM-S/IMHS OFF-AXIS COMPOSITE.

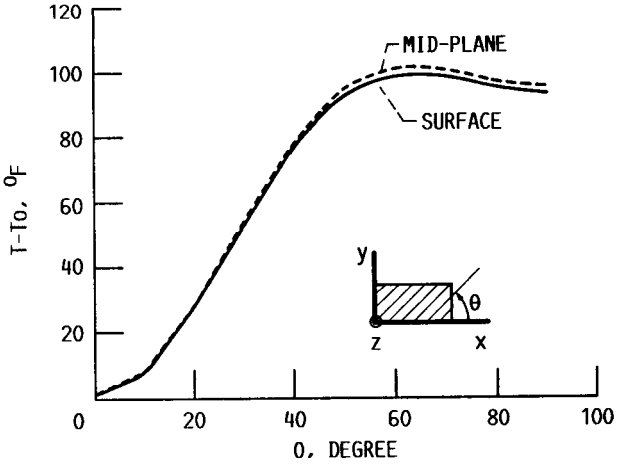

FIGURE 12. - TEMPERATURE RISE IN A 50 PERCENT HT-S/IMHS OFF-AXIS COMPOSITE SUBJECTED TO CONTINUOUS SINUSOIDAL EXCITATION.

NASA
National Aeronautics and Space Administration

Report Documentation Page

1. Report No.	2. Government Accession No.	3. Recipient's Catalog No.
NASA TM-102107		

4. Title and Subtitle	5. Report Date
Unified Micromechanics of Damping for Unidirectional Fiber Reinforced Composites	August 1989
	6. Performing Organization Code

7. Author(s)	8. Performing Organization Report No.
D.A. Saravanos and C.C. Chamis	E-4874
	10. Work Unit No.
	505-63-11

9. Performing Organization Name and Address	11. Contract or Grant No.
National Aeronautics and Space Administration Lewis Research Center Cleveland, Ohio 44135-3191	
	13. Type of Report and Period Covered
	Technical Memorandum

12. Sponsoring Agency Name and Address	14. Sponsoring Agency Code
National Aeronautics and Space Administration Washington, D.C. 20546-0001	

15. Supplementary Notes

D.A. Saravanos, National Research Council--NASA Research Associate.

16. Abstract

An integrated micromechanics methodology for the prediction of damping capacity in fiber-reinforced polymer matrix unidirectional composites has been developed. Explicit micromechanics equations based on hysteretic damping are presented relating the on-axis damping capacities to the fiber and matrix properties and volume fraction. The damping capacities of unidirectional composites subjected to off-axis loading are synthesized from on-axis damping values. Predicted values correlate satisfactorily with experimental measurements. The hygro-thermal effect on the damping performance of unidirectional composites due to temperature and moisture variations is also modeled. The damping contributions from interfacial friction between broken fibers and matrix are incorporated. Finally, the temperature rise in continuously vibrating composite plies is estimated. Application examples illustrate the significance of various parameters on the damping performance of unidirectional and off-axis fiber reinforced composites.

17. Key Words (Suggested by Author(s))	18. Distribution Statement
Composites; In-plane damping; Out-of-plane damping; Temperature effects; Moisture effects; Off-axis damping; Broken-fiber effects; Temperature rise	Unclassified - Unlimited Subject Category 24

19. Security Classif. (of this report)	20. Security Classif. (of this page)	21. No of pages	22. Price*
Unclassified	Unclassified	26	A03

*For sale by the National Technical Information Service, Springfield, Virginia 22161